

# Antibody-modified integrated microfluidic terahertz biosensor for detection of breast cancer biomarkers\*

LIU Jianjun\*\*

*School of Intelligent Engineering, Shaoguan University, Shaoguan 512005, China*

(Received 20 June 2023; Revised 4 October 2023)

©Tianjin University of Technology 2024

Breast cancer is the most common malignant tumor in women, which seriously threatens the physical and mental health of women worldwide. The existing detection methods have problems, such as large sample consumption, time-consuming sample preparation, expensive equipment, and low sensitivity. In order to solve these problems, this paper proposes a method for quickly detecting breast cancer using surface-functionalized terahertz metamaterial biosensors. The use of PIK3CA-modified sensors enhances the detection sensitivity and specificity of exosomes. Based on the red shift of the sensor absorption peak caused by exosomes, breast cancer patients can be distinguished from healthy controls. This study demonstrates that exosome detection is effective for the repeatable and non-invasive diagnosis of breast cancer patients. The terahertz metamaterial biosensor designed in this paper has high specificity, repeatability, and sensitivity, and has great potential for application in the development of modern diagnostic instruments.

**Document code:** A **Article ID:** 1673-1905(2024)04-0249-8

**DOI** <https://doi.org/10.1007/s11801-024-3109-2>

In recent years, exosomes have become a powerful diagnostic tool for breast cancer as they can be isolated from bodily fluids and carry a large amount of molecular information, particularly proteins from parent cells<sup>[1-4]</sup>. These proteins include important biological markers for cell metabolism, immune response, cancer progression, and cancer metastasis<sup>[5-9]</sup>. Generally, cancer cells produce and release more exosomes than normal cells, and the molecules contained in exosomes from tumor cells are significantly different from those in normal cells.

To validate the potential of plasma exosomes as a novel biomarker for monitoring breast cancer, current research investigates whether terahertz metamaterial biosensors can detect KRAS mutations, PIK3CA, and BRAF in plasma exosomes from breast cancer patients. KRAS mutations are associated with approximately 40% of breast cancer cases<sup>[10-12]</sup>. Breast cancer cells release more exosomes with altered protein composition in the presence of KRAS. These exosomes transfer their protein cargo to nearby KRAS wild-type cells, significantly stimulating their growth<sup>[13]</sup>, indicating the presence of components in exosomes that may indicate KRAS mutations in breast cancer cells. Therefore, various studies have identified it as a clinical prognostic and predictive marker for breast cancer<sup>[14,15]</sup>. However, the existing detection methods have some problems, such as large sam-

ple consumption, time-consuming sample preparation, expensive equipment and low sensitivity. Terahertz metamaterial biosensor is an effective method for trace bio-molecule detection because of its strong resonant interaction with bio-molecules.

Terahertz time domain spectroscopy is a cutting-edge technology, which has potential applications in unmarked nondestructive testing and analysis of biomaterials<sup>[16-20]</sup>, medical testing<sup>[21-23]</sup> and substance identification<sup>[24]</sup>. CONG et al<sup>[25]</sup> designed a highly sensitive terahertz biomolecule sensor, which has an order of magnitude higher quality factor than the conventional planar sensor. ZHANG et al<sup>[26]</sup> used the terahertz sensor to detect apoptosis in real time and found that the resonant frequency of the sensor varies linearly with the number of cells on the surface, because the number of cells will affect the equivalent dielectric constant of the surface environment of the sensor. GENG et al<sup>[27]</sup> used microfluidics to enhance the sensitivity in the terahertz range. The sensitivity is 1 700 nm/RIU and the figure of merit (*FOM*) value is 283.3.

LIU et al<sup>[28]</sup> proposed a high performance refractive index sensor based on polarization insensitive Fano, whose *FOM* and *Q* values are 721 and 5 126, respectively, which provides a new way to achieve more accurate biological detection. WANG et al<sup>[29]</sup> demonstrated a

\* This work has been supported by the Natural Science Foundation of Guangdong Province (No.2022A1515011409), the Youth Project of National Natural Science Foundation of China (Nos.52105268 and 62001200), the Science and Technology Program of Shaoguan (Nos.2019sn056, 2019sn066 and 200811094530811), the Key Project of Shaoguan University (Nos.SZ2017KJ08 and SZ2020KJ02), and the Natural Science Foundation of Fujian Province (No.2020J01817).

\*\* E-mail: liujianjun8888@hotmail.com

terahertz metamaterial biosensor for the detection of exosomes and proposed a new method for rapid diagnosis of colorectal cancer. DAI et al<sup>[30]</sup> proposed a terahertz metal-graphene composite supersensor for the detection of chlorothalonil solution. This study opened up a new way for the development of ultra-sensitive terahertz sensors and has a wide application prospect in the fields of environmental monitoring and food safety. MU et al<sup>[31]</sup> proposed a terahertz metal surface sensor based on nanometer silver (AgNPs) integration, and applied it to improve the sensitivity of material detection. The enhancement of local electric field excited by AgNPs can greatly enhance the interaction between terahertz wave and analyte, thus improving the detection sensitivity. ZHAO et al<sup>[32]</sup> proposed a strategy to identify substances by correlating the peak value of the fingerprint with the resonance frequency shift of the metamaterial sensor. This study established the relationship between the resonance frequency shift of the sensor and the fingerprint peak of the substance. Therefore, within a certain range of some unknown substances, the fingerprint peak position of these substances can be inferred from the frequency shift of the sensor. This study provides a new idea for the specific detection of substances by metamaterial sensors.

Although the above research results preliminarily show the potential of terahertz spectroscopy in the detection of tumor cells, in most cases, it is difficult to avoid the interference of the detection signal by the culture medium around the cell sample. The main component of the culture medium around living cells is water molecules, which is the necessary environment for most cells to produce, but because water molecules are polar molecules, the absorption of terahertz waves is very strong. Therefore, the main components of the cell sample and the surrounding medium are water molecules, that is to say, the cell signal and the signal of the surrounding medium are dominated by water molecules.

Based on existing research, this paper proposes an antibody-modified terahertz microfluidic biosensor for the detection and analysis of cancer exosomes. The experimental results were analyzed in terms of detection ability, detection specificity, and detection sensitivity, confirming the detection principle and efficacy of the terahertz microfluidic biosensor. Antibody modification was performed on the terahertz microfluidic biosensor to carry out detection experiments targeting breast cancer markers.

In the pathological report of breast cancer, the results of immunohistochemical detection can identify the molecular type of breast cancer, guide the treatment and indicate the prognosis. The related immunohistochemical indexes of molecular types commonly used in the diagnosis of breast cancer are PIK3CA antibody, Ki-67, HER-2, ER, PR and so on. These indicators provide a basis for later treatment. Therefore, this paper takes PIK3CA antibody, Ki-67, HER-2, ER, PR as the research

object. The PIK3CA antibody, Ki-67, HER-2, ER and PR are purchased from Beijing Yiqiao Shenzhou Company. Chloroauric acid hydrate, sodium citrate, anhydrous ethanol, 3-aminopropyltriethoxysilane (APTES), HS-PEG-COOH, 1-ethyl-3-(3-dimethylaminopropyl) carbodiimide hydrochloride (EDC), N-hydroxysuccinimide (NHS), phosphate-buffered saline (PBS, pH=7.4) were purchased from Aladdin Company. The plasma exosome extraction kit was purchased from Umibio Company. In this study, 16 plasma samples were provided by the Department of Oncology, Medical School of Shaoguan University. Among them, 10 samples were taken from patients diagnosed with breast cancer based on imaging and pathological diagnosis, and 6 plasma samples were taken from healthy individuals.

The terahertz time-domain spectroscopy system used in this study consists of a pump light source (fiber femtosecond laser, TOPTICA Photonics, Germany) and a terahertz time-domain spectroscopy optical path system (Z3-XL, Zomega, USA), as shown in Fig.1. The detection modes of the spectroscopy system include transmission, reflection, and attenuated total reflection. The fiber femtosecond laser generates a laser with a center wavelength of 800 nm, pulse width of <100 fs, repetition rate of 80 MHz, and output power of 140 mW. The system can measure the basic optical parameters of samples, has fully autonomous testing and analysis software, provides real-time online measurement results, and has a spectral range from 0.1 THz to 3.5 THz. Fig.1 shows a schematic diagram of the principle of the terahertz time-domain spectroscopy system.

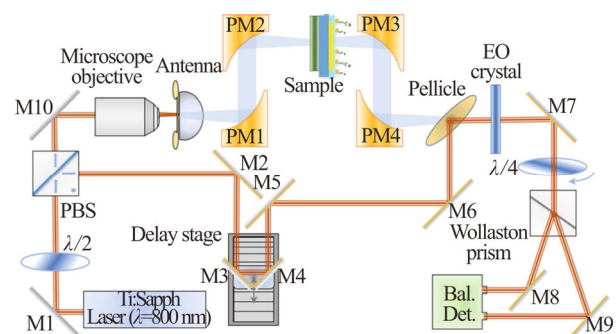


**Fig.1 Transmittance detection mode of terahertz time-domain spectroscopy system**

Fig.2(a) illustrates the unit structure of a terahertz microflow biosensor with a metamaterial absorber. The sensor is composed of five layers, namely the dielectric layer, the metal microstructure, the microflow channel, the metal reflector, and the substrate, from top to bottom. The dielectric layer is made of quartz material with a dielectric constant of  $3.75+i0.015$  and a thickness of  $4\ \mu\text{m}$ . The metal layer and metal reflector are both made of gold material with a conductivity of  $4.52\times 10^7\ \text{S/m}$  and a thickness of  $0.1\ \mu\text{m}$ . The substrate is made of silicon material with a dielectric constant of  $11.9$  and a thickness of  $50\ \mu\text{m}$ , which does not impact the performance of the

sensor. The period of the unit structure, denoted as  $l_1$ , is 120  $\mu\text{m}$ . The microfluidic channel is located between the metal reflector and metal microstructure, and its height is denoted as  $h_3$ , which is equal to 5  $\mu\text{m}$ . The metal microstructure of the sensor consists of a double-ring structure, as shown in Fig.2(b). The optimized geometric parameters of the structure are presented in Tab.1.

According to the sample diagram of Fig.2(b), the photoresist is etched on the substrate by S1813/LOR double-layer photoresist, the pattern on the template is transferred to the photoresist substrate by MA6 exposure machine and CD26 development, the metal silver is uniformly deposited on the open ring resonator pattern of the high resistance P-type silicon substrate by the thermal evaporation deposition system, and the double-ring structure sample of the high resistance P-type silicon deposited metal silver is obtained by stripping (lift-off) process. Fig.2(c) shows a panoramic view of the sample of the double-ring metamaterial absorber under a high-power microscope.

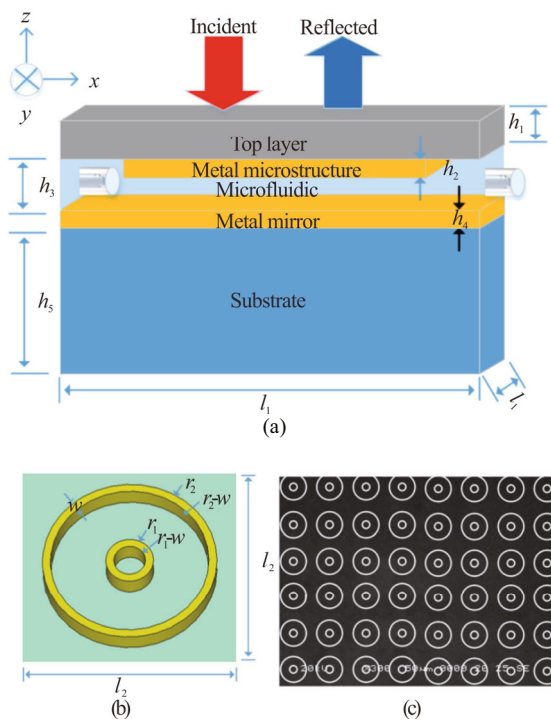


**Fig.2 Schematic diagram of the terahertz microfluidic sensor structure: (a) Side view of the unit structure; (b) Metal microstructure unit; (c) Panoramic view under high-power microscope**

**Tab.1 Geometric parameters of terahertz microfluidic sensor structure unit**

Parameters	$l_1$	$r_1$	$r_2$	$w$	$h_1$	$h_2$	$h_3$	$h_4$	$h_5$
Value ( $\mu\text{m}$ )	120	100	40	5	4	0.1	5	0.1	50

In this study, the three-dimensional electromagnetic field simulation software CST was used to perform cal-

culations and simulations on the metal resonant structure column using the finite difference time domain method. During the simulation, the  $x$  and  $y$  directions were set as cell boundary conditions, while the  $z$  direction was set as an open boundary condition<sup>[18]</sup>. Fig.3(a) shows the impact of the refractive index ( $n$ ) of the analyte increasing from 1.0 to 2.0 on the terahertz metamaterial biosensor under the condition of a microfluidic channel height of  $h_3=5 \mu\text{m}$ , and the corresponding change in resonance frequency with varying refractive index is shown in Fig.3(b). Both low and high resonance frequencies are highly sensitive to changes in the microenvironment. At the low frequency ( $f_L=0.453 \text{ THz}$ ), the sensitivity of the metal resonant structure is 186 GHz/RIU, while at the high frequency ( $f_H=1.03 \text{ THz}$ ), the sensitivity of the metal resonant structure is 258 GHz/RIU. Therefore, in this study, the high-frequency resonance point, which has higher sensitivity, was used to characterize the reaction between the antibody and extracellular vesicles.

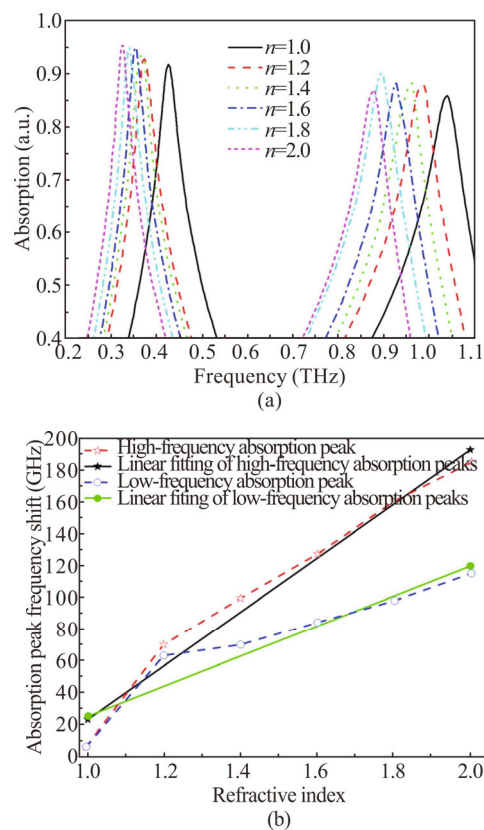


**Fig.3 (a) Terahertz absorption spectra of air-biosensor under different refractive index conditions; (b) Relationship between refractive index and frequency shift of high- and low-frequency absorption peaks**

To apply the terahertz metamaterial biosensor to the analysis of breast cancer extracellular vesicle expression, this study used antibodies for specific functionalization. The basic process of detecting extracellular vesicles using the antibody-modified terahertz metamaterial biosensor is shown in Fig.4.

To verify the effectiveness of the surface functionalization process of the sensor, this study analyzed the terahertz absorption spectra of three states: without antibody modification, with antibody modification, and with antibody modification plus extracellular vesicles (as shown in Fig.5(a)). It can be observed that the terahertz absorption spectra of the metamaterial biosensor with antibody modification had a significant red shift compared to the

biosensor without antibody modification, especially when extracellular vesicles were added on the antibody-modified biosensor. The red shift phenomenon of the terahertz absorption spectra indicates that the surface functionalization process of the sensor through antibody modification in this paper is effective, which provides a basis for subsequent specific recognition detection experiments.

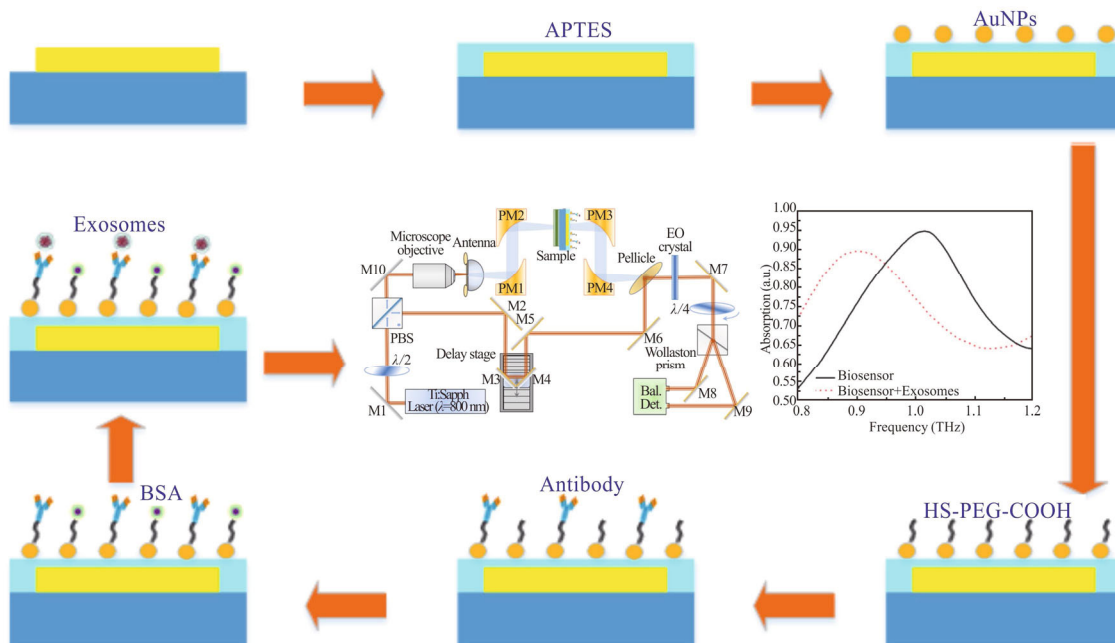


Fig.4 Flowchart of biosensor functionalization process

The detection capability of the terahertz metamaterial biosensor determines whether the sensor can accurately measure the target substance. Therefore, this study conducted a detection capability test on the designed terahertz biosensor. Fig.6(a) shows the terahertz absorption spectra of the sensor before and after antibody modification in detecting extracellular vesicle samples. It can be observed that the terahertz absorption spectra underwent a red shift. By enlarging the high-frequency absorption peak (Fig.6(b)), it can be found that the high-frequency absorption resonance peak shifted by 63 GHz before and after adding extracellular vesicle samples to the sensor

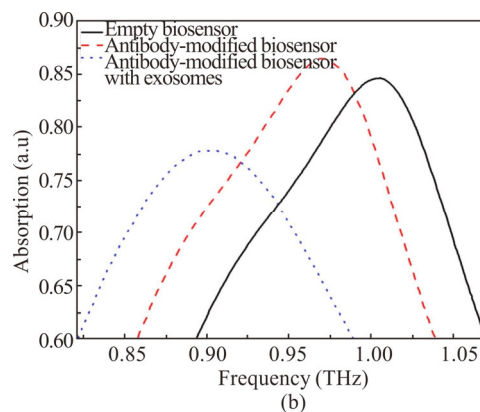
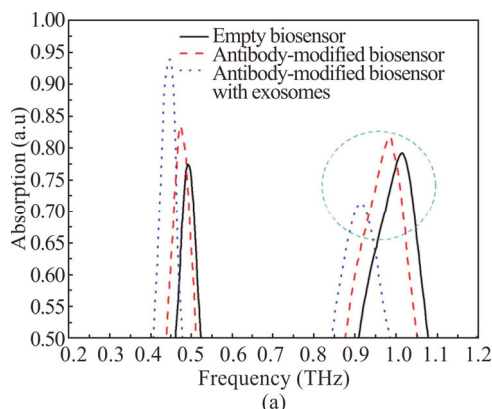
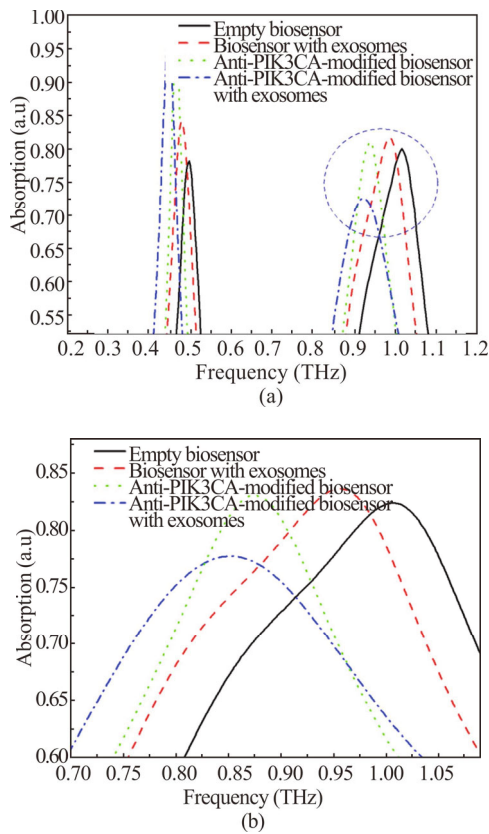


Fig.5 (a) Comparison of absorption spectra between surface-functionalized terahertz metamaterial biosensor and bare biosensor; (b) Local amplification of high-frequency absorption peak

without antibody modification, while the high-frequency absorption resonance peak shifted by 62 GHz before and after adding extracellular vesicle samples to the sensor with antibody modification. The experimental results analysis indicates that the designed terahertz metamaterial biosensor and antibody modification method in this paper are effective.

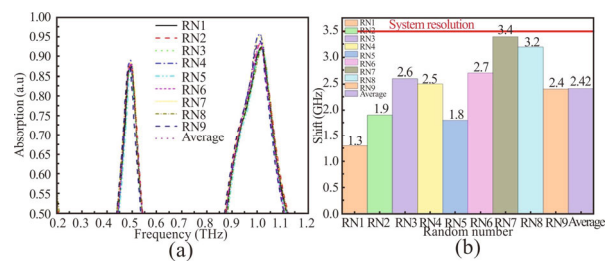


**Fig.6 (a) Absorption spectra of bare biosensor and biosensor modified with PIK3CA antibodies before and after adding extracellular vesicle samples; (b) Local amplification of high-frequency absorption peak**

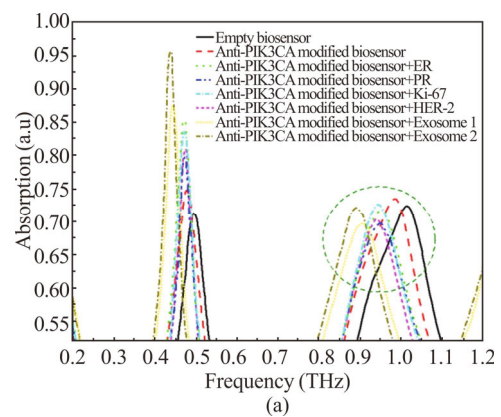
The reproducibility of the terahertz metamaterial biosensor determines whether the sensor can reproduce the same measurement results accurately and ensure the reliability and accuracy of experimental results. Therefore, this study conducted a reproducibility test on the designed terahertz biosensor, and the results are shown in Fig.7(a). RN1 to RN10 in Fig.7 represent the randomly selected times the sensor was used, and "Average" is the data average of the biosensor. Fig.7(b) shows the column chart of the red shift of the high-frequency resonance peak. It can be seen that the high-frequency peak underwent red shifts of 1.3 GHz, 1.9 GHz, 2.6 GHz, 2.5 GHz, 1.8 GHz, 2.7 GHz, 3.4 GHz, 3.2 GHz, and 2.4 GHz. The average frequency shift of the high-frequency resonance peak of the sensor after multiple cleanings was 2.42 GHz, while the accuracy of the terahertz time-domain spectroscopy system used in this paper is 3.5 GHz. Therefore, the designed terahertz metamaterial biosensor in this paper has good reproducibility.

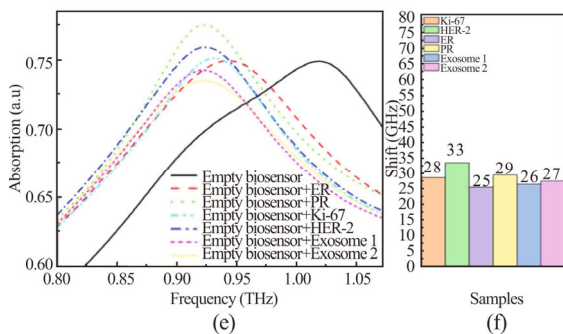
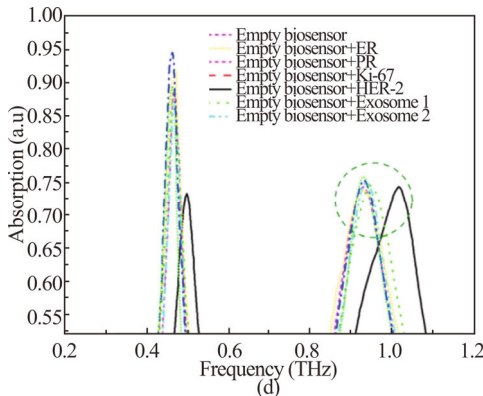
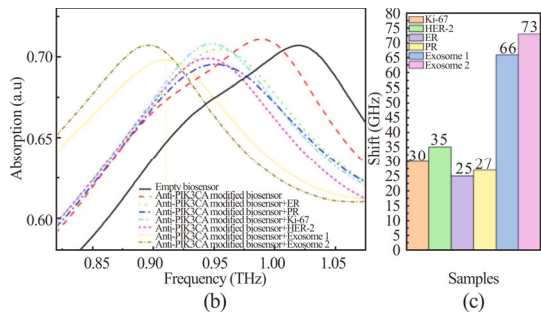
To verify the correctness, accuracy, and reliability of the information obtained by the sensor on the target substance, this study added Ki-67, HER-2, ER, PR, and extracellular vesicle samples to the biosensor modified with PIK3CA antibodies and verified its specificity by ana-

lyzing the terahertz absorption spectra characteristics of the sensor. The obtained terahertz absorption spectra of each sample are shown in Fig.8(a). It can be observed from the local amplification of the high absorption peak (Fig.8(b)) that after adding different detection samples to the biosensor modified with PIK3CA antibodies, the terahertz absorption resonance peaks all underwent varying degrees of red shifts. As shown in Fig.8(c), the high-frequency resonance peaks produced red shifts of 30 GHz, 35 GHz, 25 GHz, 27 GHz, 66 GHz, and 73 GHz, respectively. The smallest resonance frequency shift of the extracellular vesicle sample is 45% higher than that of the other four detection substances, and the largest resonance frequency shift of the extracellular vesicle sample is 53% higher than that of the other four detection substances. Therefore, the biosensor modified with PIK3CA antibodies has the ability to detect extracellular vesicles (with high specificity). To make a comparison, the terahertz transmission spectra of the sensor without antibody modification after adding different detection samples are shown in Fig.8(d). It can be found from the local amplification of the high absorption peak (Fig.8(e)) that the high-frequency absorption peak red shifts of each extracellular vesicle sample are similar to those of other detection samples, producing red shifts of 28 GHz, 33 GHz, 25 GHz, 29 GHz, 26 GHz, and 27 GHz, respectively (Fig.8(f)). Therefore, the biosensor without antibody modification does not have the ability to detect extracellular vesicles, while the biosensor modified with PIK3CA antibodies has high specificity.



**Fig.7 (a) Absorption peak spectra of the biosensor obtained multiple times randomly; (b) Bar chart of high-frequency absorption peak shift**

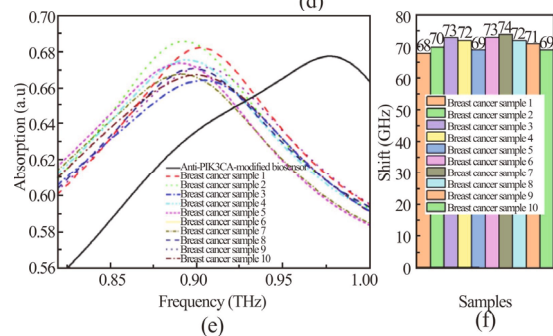
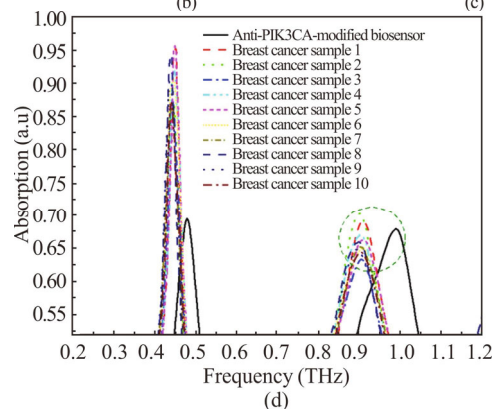
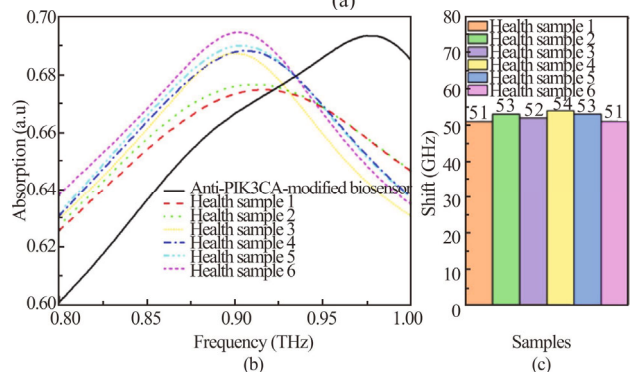
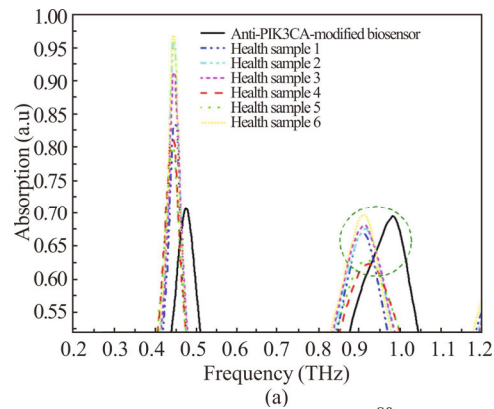




**Fig.8 (a) Terahertz absorption spectra of the biosensor modified with PIK3CA antibodies for different samples; (b) Local amplification of high-frequency absorption peak of terahertz spectrum for the biosensor modified with antibodies; (c) Bar chart of red shift of high-frequency absorption peak for different samples (with antibody modification); (d) Terahertz absorption spectra of the biosensor without antibody modification for different samples; (e) Local amplification of high-frequency absorption peak of terahertz spectrum for the biosensor without antibody modification; (f) Bar chart of red shift of high-frequency absorption peak for different samples (without antibody modification)**

To test the biosensor modified with PIK3CA antibodies for detecting breast cancer, extracellular vesicle samples from breast cancer patients (breast cancer samples 1—10) and healthy controls (health samples 1—6) were tested. The obtained absorption spectra and corresponding resonance frequency shift results are shown in Fig.9(a)—(c), and the detection results of extracellular vesicle samples from breast cancer patients show resonance frequency shifts between 68 GHz and 74 GHz.

The detection results of extracellular vesicle samples from healthy controls show resonance frequency shifts between 51 GHz and 54 GHz (Fig.9(d)—(f)). As shown in Fig.9(g), setting the detection threshold to 60 GHz, resonance frequency shifts below 60 GHz can be identified as healthy, while resonance frequency shifts above 60 GHz can be identified as breast cancer. Therefore, the biosensor modified with PIK3CA antibodies proposed in this study can distinguish extracellular vesicles from breast cancer patients and healthy controls.



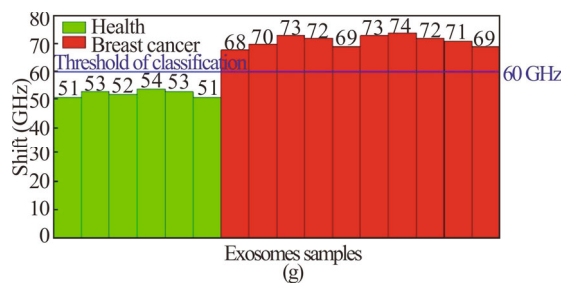


**Fig.9** (a) Terahertz absorption spectra of the biosensor modified with PIK3CA antibodies for healthy samples detection; (b) Local amplification of high-frequency absorption peak of terahertz spectrum for healthy sample; (c) Bar chart of red shift of high-frequency absorption peak for healthy sample; (d) Terahertz absorption spectra of the biosensor modified with PIK3CA antibodies for breast cancer sample detection; (e) Local amplification of high-frequency absorption peak of terahertz spectrum for breast cancer sample; (f) Bar chart of red shift of high-frequency absorption peak for breast cancer sample; (g) Bar chart of red shift of high-frequency absorption peak (PIK3CA mutation)

In this study, a method for rapid detection of breast cancer using surface-functionalized terahertz metamaterial biosensors was proposed. The biosensor has two absorption peaks, with the high-frequency absorption peak being more sensitive to changes in the surface medium environment. Therefore, the high-frequency absorption peak was selected to characterize the reaction between extracellular vesicles and antibodies for detection. By modifying the terahertz biosensor with PIK3CA antibodies, the designed biosensor has higher detection sensitivity and specificity for extracellular vesicles. Based on the red shift of the sensor absorption peak caused by extracellular vesicles, breast cancer patients can be distinguished from healthy controls. This research demonstrates that extracellular vesicle detection is effective for non-invasive diagnosis and repeatability of breast cancer patients, and surface-functionalized terahertz metamaterial biosensors have great potential in the development of modern clinical diagnostic instruments and pharmacological equipment with high repeatability, specificity, and sensitivity.

### Ethics declarations

### Conflicts of interest

The authors declare no conflict of interest.

### References

- [1] DOYLE L M, WANG M Z. Overview of extracellular vesicles, their origin, composition, purpose, and methods for exosome isolation and analysis[J]. *Cells*, 2019, 8(7): 727.
- [2] IANG K, LIU F, FAN J, et al. Nanoplasmonic quantifi-

cation of tumour-derived extracellular vesicles in plasma microsamples for diagnosis and treatment monitoring[J]. *Nature biomedical engineering*, 2017, 1(4): 0021.

- [3] CHEN I, XUE L, HSU C, et al. Phosphoproteins in extracellular vesicles as candidate markers for breast cancer[J]. *Proceedings of the national academy of sciences*, 2017, 114(12): 3175-3180.
- [4] KOWAL J, ARRAS G, COLOMBO M, et al. Proteomic comparison defines novel markers to characterize heterogeneous populations of extracellular vesicle subtypes[J]. *Proceedings of the national academy of sciences of the United States of America*, 2016, 113(8): E968-E977.
- [5] WANG L, DENG Y, HUANG Y, et al. Template-free multiple signal amplification for highly sensitive detection of cancer cell-derived exosomes[J]. *Chemical communications*, 2021, 57(68): 8508-8511.
- [6] SUN Z, WANG L, WU S, et al. An electrochemical biosensor designed by using Zr-based metal organic frameworks for the detection of glioblastoma-derived exosomes with practical application[J]. *Analytical chemistry*, 2020, 92(5): 3819-3826.
- [7] WANG L, PAN Y, LIU Y, et al. Fabrication of an aptamer-coated liposome complex for the detection and profiling of exosomes based on terminal deoxynucleotidyl transferase-mediated signal amplification[J]. *ACS applied materials and interfaces*, 2020, 12(1): 322-329.
- [8] PAN Y, WANG L, DENG Y, et al. A simple and sensitive method for exosome detection based on steric hindrance-controlled signal amplification[J]. *Chemical communications*, 2020, 56(89): 13768-13771.
- [9] WANG L, YANG Y, LIU Y, et al. Bridging exosome and liposome through zirconium-phosphate coordination chemistry: a new method for exosome detection[J]. *Chemical communications*, 2019, 55(18): 2708-2711.
- [10] WANG L, DENG Y, WEI J, et al. Spherical nucleic acids-based cascade signal amplification for highly sensitive detection of exosomes[J]. *Biosensors and bioelectronics*, 2021, 191: 113465.
- [11] WANG M H, PAN Y H, WU S, et al. Detection of colorectal cancer-derived exosomes based on covalent organic frameworks[J]. *Biosensors and bioelectronics*, 2020, 169: 112638.
- [12] SHANG A, GU C, ZHOU C, et al. Exosomal KRAS mutation promotes the formation of tumor-associated neutrophil extracellular traps and causes deterioration of colorectal cancer by inducing IL-8 expression[J]. *Cell communication and signaling*, 2020, 18(1): 52.
- [13] ROOCK W D, VRIENDT V D, NORMANNO N, et al. KRAS, BRAF, PIK3CA, and PTEN mutations: implications for targeted therapies in metastatic colorectal cancer[J]. *Lancet oncology*, 2011, 12(6): 594-603.
- [14] ZHOU C, SUN H, ZHENG C, et al. Oncogenic HSP60 regulates mitochondrial oxidative phosphorylation to support Erk1/2 activation during pancreatic cancer cell growth[J]. *Cell death and disease*, 2018, 9(2): 161.

- [15] CAMPANELLA C, RAPPA F, SCIUMÈ C, et al. Heat shock protein 60 levels in tissue and circulating exosomes in human large bowel cancer before and after ablative surgery[J]. *Cancer*, 2015, 121(18): 3230-3239.
- [16] YAN X, YANG M S, ZHANG Z, et al. The terahertz electromagnetically induced transparency-like metamaterials for sensitive biosensors in the detection of cancer cells[J]. *Biosensors and bioelectronics*, 2018, 126: 485-492.
- [17] ZHAO R, ZOU B, ZHANG G L, et al. High-sensitivity identification of aflatoxin B1 and B2 using terahertz time-domain spectroscopy and metamaterial-based terahertz biosensor[J]. *Journal of physics D: applied physics*, 2020, 53(19): 195401.
- [18] LI B, ZHAO X, ZHANG Y, et al. Prediction and monitoring of leaf water content in soybean plants using terahertz time-domain spectroscopy[J]. *Computers and electronics in agriculture*, 2020, 170(2): 105239.
- [19] ZHU Z, CHENG C, CHANG C, et al. Characteristic fingerprint spectrum of neurotransmitter norepinephrine with broadband terahertz time-domain spectroscopy[J]. *Analyst*, 2019, 144(8): 2504-2510.
- [20] CHEN K, XU D G, LI J N, et al. Application of terahertz time-domain spectroscopy in atmospheric pressure plasma jet diagnosis[J]. *Results in physics*, 2020, 16: 102928.
- [21] CHEN H, CHEN T H, TSENG T F, et al. High-sensitivity in vivo THz transmission imaging of early human breast cancer in a subcutaneous xenograft mouse model[J]. *Optics express*, 2011, 19(22): 21552-21562.
- [22] LIU Y, LIU H, TONG M Q, et al. The medical application of terahertz technology in non-invasive detection of cells and tissues: opportunities and challenges[J]. *RSC advances*, 2019, 9(17): 9354-9363.
- [23] HIDAYAT M V, APRIONO C. Simulation of terahertz imaging using microstrip linear array antenna for breast cancer detection[J]. *AIP conference proceedings*, 2019, 2092: 020020.
- [24] YUMA T, KOUJI N, HIROAKI M. Security screening system based on terahertz-wave spectroscopic gas detection[J]. *Optics express*, 2020, 29(2): 2529-2537.
- [25] CONG L, TAN S, YAHIAOUI R, et al. Experimental demonstration of ultrasensitive sensing with terahertz metamaterial absorbers: a comparison with the metasurfaces[J]. *Applied physics letters*, 2015, 106(3): 26.
- [26] ZHANG C H, LIANG L J, DING L, et al. Label-free measurements on cell apoptosis using a terahertz metamaterial-based biosensor[J]. *Applied physics letters*, 2016, 108(24): 209-223.
- [27] GENG Z, ZHANG X, FAN Z, et al. A route to terahertz metamaterial biosensor integrated with microfluidics for liver cancer biomarker testing in early stage[J]. *Scientific reports*, 2017, 7(1): 16378.
- [28] LIU H G, ZHENG L, MA P Z, et al. Metasurface generated polarization insensitive Fano resonance for high-performance refractive index sensing[J]. *Optics express*, 2019, 27(9): 13252-13262.
- [29] WANG Y, WANG Y, HU F, et al. Surface-functionalized terahertz metamaterial biosensor used for the detection of exosomes in patients[J]. *Langmuir*, 2022, 38(12): 3739-3747.
- [30] DAI Z, YANG M, MOU T, et al. Tracing pictogram-level chlorothalonil pesticide based on terahertz metal-graphene hybrid metasensors[J]. *Optics communications*, 2023, 529: 129025.
- [31] MU T, YE Y, DAI Z, et al. Silver nanoparticles-integrated terahertz metasurface for enhancing sensor sensitivity[J]. *Optics express*, 2022, 30(23): 41101-41109.
- [32] ZHAO R, YE Y, DAI Z, et al. Research on specific identification method of substances through terahertz metamaterial sensors[J]. *Results in physics*, 2022, 43: 106055.